

A mixed finite-element scheme of a semiconductor energy-transport model using dual entropy variables

Stephan Gadau, Ansgar Jüngel, and Paola Pietra

ABSTRACT. One-dimensional stationary energy-transport equations for semiconductors in the dual entropy variable formulation are numerically discretized employing a mixed-hybrid finite-element method which has the advantage to fulfill current conservation. Numerical results for two ballistic diodes are presented and numerical convergence rates are computed.

1. Introduction

The simulation of modern ultra-small semiconductor devices requires the use of advanced models which are able to deal with physical effects such as carrier heating and velocity overshoot. The energy-transport equations seem to provide a reasonable compromise between physical accuracy and numerical efficiency. They consist of the conservation laws of mass and energy for the electron density n and electron temperature T , together with constitutive relations for the particle and energy fluxes J_1 and J_2 , respectively, and are coupled to the Poisson equation for the electrostatic potential V . In one space dimension, the scaled stationary equations read as follows:

$$\begin{aligned} (1.1) \quad & -\partial_x J_1 = 0, & J_1 &= \partial_x n - T^{-1} n \partial_x V, \\ (1.2) \quad & -\partial_x J_2 = -J_1 \partial_x V + W(n, T), & J_2 &= \frac{3}{2} \partial_x (nT) - \frac{3}{2} n \partial_x V, \\ (1.3) \quad & \lambda^2 \partial_{xx} V = n - C(x), & x \in I &= (0, 1). \end{aligned}$$

Here, $W(n, t) = 3n(1 - T)/2\tau$ is the relaxation term with the (scaled) energy relaxation time τ , λ denotes the scaled Debye length, and $C(x)$ is the doping profile (see [13] for details). The equations are completed by the boundary conditions

$$(1.4) \quad n(0) = n(1) = 1, \quad T(0) = T(1) = 1, \quad V(0) = U, \quad V(1) = 0.$$

This energy-transport model has been derived in [2, 6] from the semiconductor Boltzmann equation by means of a Hilbert expansion method and is referred to

as the *Chen model* since it has been used by Chen et al. in [4]. The first energy-transport model has been presented by Stratton [20].

The derivation in [2] provides another formulation of the energy-transport equations, namely in the *primal entropy variables* μ/T and $-1/T$, where μ is the chemical potential, related to the particle density by the expression $n(\mu, T) = N_0 T^{3/2} \exp(\mu/T)$, $N_0 > 0$ being a scaled density. Although this formulation makes clear the connection to thermodynamics, the equations still contain the Joule heating term $-J_1 \partial_x V$ in (1.2) and are convection dominated, which complicates the numerical approximation. In [1, 5] it has been observed that the Joule heating term vanishes if the *dual entropy variables* $w_1 = (\mu - V)/T$ and $w_2 = -1/T$ are employed. In these variables, the equations (1.1) and (1.2) become

$$(1.5) \quad -\partial_x I_1 = 0, \quad I_1 = D_{11} \partial_x w_1 + D_{12} \partial_x w_2,$$

$$(1.6) \quad -\partial_x I_2 = W(n, T), \quad I_2 = D_{21} \partial_x w_1 + D_{22} \partial_x w_2,$$

where the diffusion coefficients are given by

$$D_{11} = n, \quad D_{12} = D_{21} = -n \left(V + \frac{3}{2} T \right), \quad D_{22} = n \left(V - \frac{3}{2} T \right)^2 + \frac{3}{2} n T^2.$$

The main objective of this paper is to present a numerical scheme for the strongly coupled elliptic problem (1.4)-(1.6) in the dual entropy variables w_1, w_2 .

The numerical discretization of energy-transport models has been investigated in the physical literature for quite some years (see, e.g., [4, 7, 19]). Mathematicians employed ENO (essentially non-oscillatory) schemes [12], finite-difference methods [8], mixed finite volumes [3], and mixed finite elements [9, 10, 14, 17, 18].

More precisely, the authors in [9] employed a mixed-hybrid finite-element method for (1.1)-(1.2), taking advantage of the drift-diffusion type formulation of the current expressions. Since zero-order terms are taken into account, the use of standard mixed finite elements generally does not provide an M-matrix which is desirable in view of a discrete maximum principle. In order to guarantee the M-matrix property, finite elements developed in [15, 16] have been used instead.

Another approach has been presented in [17, 18]. The authors of [17, 18] are working in the dual entropy variable formulation and employ a standard mixed finite-element scheme together with an artificial time derivative. The disadvantage of this approach is that a large discrete system has to be solved.

In this paper, we also work with dual entropy variables, but we employ a *hybridized form* of the mixed finite-element method. Compared to [9], we can use standard finite elements which are easier to handle than the finite elements of [16] but still provide the M-matrix property. Compared to [17], we can apply static condensation to the algebraic system which allows to reduce the complexity of the discrete problem considerably.

The paper is organized as follows. The mixed-hybrid finite-element discretization of problem (1.4)-(1.6) is presented in section 2. In section 3 two one-dimensional ballistic diodes which can be considered as a benchmark model are simulated and

numerical convergence rates are given. The extension of this approach to two space dimensions is in preparation.

2. Discretization of the equations

We choose an equidistant grid $x_i = ih$, $i = 0, \dots, N$, and the discretization parameter $h = 1/N$. Furthermore, we introduce the following finite-element spaces:

$$\begin{aligned} X_h &= \{f \in L^2(I) : f \text{ is linear on } (x_{i-1}, x_i) \text{ for all } i\}, \\ Y_h &= \{f \in L^2(I) : f \text{ is constant on } (x_{i-1}, x_i) \text{ for all } i\}, \\ Z_h &= \mathbb{R}^{N+1}. \end{aligned}$$

In several space dimensions, one may choose a ‘‘hybridized’’ Raviart-Thomas space of lowest order (see, e.g., [9]). Although the Poisson equation can be discretized with standard finite elements, we choose a mixed formulation also for this equation since the electric field $-\partial_x V$ is used to compute the fluxes. For this, we define the field-like variable $E = \lambda^2 \partial_x V$. The mixed-hybrid finite-element discretization of (1.3) reads as follows: Find $E_h \in X_h$, $U_h \in Y_h$, and $V_h \in Z_h$ satisfying $V_h^1 = U$, $V_h^{N+1} = 0$ (the superscripts denote components of the vector V_h) such that

$$\begin{aligned} \sum_{i=1}^N \left(\lambda^{-2} \int_{x_{i-1}}^{x_i} E_h \phi_h dx + \int_{x_{i-1}}^{x_i} U_h \partial_x \phi_h dx - [V_h \phi_h]_{x_{i-1}}^{x_i} \right) &= 0, \\ \sum_{i=1}^N \left(\int_{x_{i-1}}^{x_i} \partial_x E_h \psi_h dx - \int_{x_{i-1}}^{x_i} (n_h - C(x)) \psi_h dx \right) &= 0, \\ - \sum_{i=1}^N [\mu_h E_h]_{x_{i-1}}^{x_i} &= 0 \end{aligned}$$

for all $\phi_h \in X_h$, $\psi_h \in Y_h$, and $\mu_h \in Z_h$ satisfying $\mu_h^1 = \mu_h^{N+1} = 0$. The first equation is obtained from a weak version of $\lambda^{-2} E = \partial_x V$, using integration of parts and summation of all (x_{i-1}, x_i) . Here, E_h is an approximation of E , and both U_h and V_h approximate the potential V . The second equation is a discrete weak form of $\partial_x E = n(V, w_1, w_2) - C(x)$, and the third equation implies the continuity of E_h at the nodes. The particle density $n(V, w_1, w_2) = (-w_2)^{-3/2} \exp(w_1 - V w_2)$ is approximated by $n_h = n(\bar{V}_h^i, \bar{w}_{1h}^i, \bar{w}_{2h}^i)$, where, on each (x_{i-1}, x_i) ,

$$\bar{V}_h^i = \frac{V_h^{i-1} + V_h^i}{2}, \quad \bar{w}_{jh}^i = \frac{w_{jh}^{i-1} + w_{jh}^i}{2}, \quad j = 1, 2.$$

Before we can give the mixed-hybrid form of (1.5)-(1.6), we need some definitions. The inverse of \mathbf{D} is denoted by $\mathbf{A} = (A_{ij})_{i,j=1,2}$ (which depends on V , w_1 , and w_2), where

$$A_{11} = \frac{2w_2^2}{3n^2} D_{22}, \quad A_{12} = A_{21} = -\frac{2w_2^2}{3n^2} D_{21}, \quad A_{22} = \frac{2w_2^2}{3n^2} D_{11},$$

and set $\mathbf{A}_h = \mathbf{A}(\bar{V}_h^i, \bar{w}_{1h}^i, \bar{w}_{2h}^i)$ and $W_h = W(\bar{V}_h^i, \bar{w}_{1h}^i, \bar{w}_{2h}^i)$ on each (x_{i-1}, x_i) . Furthermore, we use the notations

$$\mathbf{I}_h = (I_{1h}, I_{2h})^\top, \quad \mathbf{v}_h = (v_{1h}, v_{2h})^\top, \quad \mathbf{w}_h = (w_{1h}, w_{2h})^\top.$$

Then, the mixed-hybrid formulation of (1.5)-(1.6) reads as follows: Find $\mathbf{I}_h \in \mathbf{X}_h = X_h^2$, $\mathbf{v}_h \in \mathbf{Y}_h = Y_h^2$, and $\mathbf{w}_h \in \mathbf{Z}_h = Z_h^2$ satisfying the boundary conditions such that

$$(2.1) \quad \sum_{i=1}^N \left(\int_{x_{i-1}}^{x_i} \phi_h \cdot \mathbf{A}_h \mathbf{I}_h \, dx + \int_{x_{i-1}}^{x_i} \mathbf{v}_h \cdot \partial_x \phi_h \, dx - [\phi_h \cdot \mathbf{w}_h]_{x_{i-1}}^{x_i} \right) = 0,$$

$$(2.2) \quad \sum_{i=1}^N \left(\int_{x_{i-1}}^{x_i} \psi_h \cdot \partial_x \mathbf{I}_h \, dx - \int_{x_{i-1}}^{x_i} \mathbf{W}_h \cdot \psi_h \, dx \right) = 0,$$

$$(2.3) \quad - \sum_{i=1}^N [\boldsymbol{\mu}_h \cdot \mathbf{I}_h]_{x_{i-1}}^{x_i} = 0$$

for all $\phi_h \in \mathbf{X}_h$, $\psi_h \in \mathbf{Y}_h$, and $\boldsymbol{\mu}_h \in \mathbf{Z}_h$ satisfying $\boldsymbol{\mu}_h^1 = \boldsymbol{\mu}_h^{N+1} = \mathbf{0}$. Equation (2.1) is derived from the weak formulation of the first equations in (1.5)-(1.6); (2.2) comes from the weak form of the second equations in (1.5)-(1.6); and finally, (2.3) imposes the continuity of the fluxes across the inter-element boundaries.

We apply static condensation in order to reduce the size of the discrete system. This yields an algebraic system for the Lagrange multipliers V_h , w_{1h} , and w_{2h} only. Locally, we can express the variables U_h , v_{1h} , v_{2h} and E_h , I_{1h} , I_{2h} in terms of the Lagrange multipliers. Indeed, we obtain

$$U_h^i = \bar{V}_h^i - \frac{h^2}{12\lambda^2}(n_h - C_h^i), \quad \mathbf{v}_h^i = \begin{pmatrix} \bar{w}_{1h}^i \\ \bar{w}_{2h}^i \end{pmatrix} - \frac{h^2}{12} \mathbf{A}_h \mathbf{W}_h,$$

where

$$C_h^i = \frac{1}{h} \int_{x_{i-1}}^{x_i} C(x) \, dx.$$

In order to derive the dependence of E_h and \mathbf{I}_h on the Lagrange multipliers, we use the local basis

$$\phi_{0i}(x) = \begin{cases} 1, & x \in (x_{i-1}, x_i) \\ 0, & \text{else,} \end{cases} \quad \phi_{1i}(x) = \begin{cases} \frac{2}{h}(x - \frac{1}{2}(x_{i-1} + x_i)), & x \in (x_{i-1}, x_i) \\ 0, & \text{else} \end{cases}$$

in X_h , since the continuity is forced by the Lagrange multipliers. On each interval (x_{i-1}, x_i) we can write $E_h = E_{0h}^i \phi_{0i} + E_{1h}^i \phi_{1i}$ and $\mathbf{I}_h = \mathbf{I}_{0h}^i \phi_{0i} + \mathbf{I}_{1h}^i \phi_{1i}$, where

$$\begin{pmatrix} E_{0h}^i \\ E_{1h}^i \end{pmatrix} = \frac{\lambda^2}{h} \mathbf{M}_h \begin{pmatrix} V_h^{i-1} \\ V_h^i \end{pmatrix} + \frac{h}{2} \begin{pmatrix} 0 \\ n_h - C_h^i \end{pmatrix},$$

$$\begin{pmatrix} \mathbf{I}_{0h}^i \\ \mathbf{I}_{1h}^i \end{pmatrix} = \frac{1}{h} \begin{pmatrix} D_{11h} \mathbf{M}_h & D_{12h} \mathbf{M}_h \\ D_{21h} \mathbf{M}_h & D_{22h} \mathbf{M}_h \end{pmatrix} \begin{pmatrix} \mathbf{w}_{1h}^i \\ \mathbf{w}_{2h}^i \end{pmatrix} + \frac{h}{2} \begin{pmatrix} \mathbf{0} \\ \mathbf{W}_h \end{pmatrix}$$

and

$$\mathbf{D}_h = \mathbf{A}_h^{-1}, \quad \mathbf{M}_h = \begin{pmatrix} -1 & 1 \\ 0 & 0 \end{pmatrix}, \quad \mathbf{w}_{jh}^i = \begin{pmatrix} w_{jh}^{i-1} \\ w_{jh}^i \end{pmatrix}, \quad j = 1, 2.$$

The nonlinear system for V_h, w_{1h}, w_{2h} is solved by a combination of the Newton and Gummel method. First, we compute the solution of the thermal equilibrium $U = 0$ as an initial guess of the iterative procedure. Then we increase the applied voltage by the voltage increment $\Delta U = 50$ mV and solve the coupled subsystem (1.5)-(1.6) using the Newton method up to convergence. Then we perform one Newton iteration step in the linearized Poisson equation,

$$(2.4) \quad \lambda^2 \partial_{xx} \delta V - n_h^{(l)} \delta V = -\lambda^2 \partial_{xx} V_h^{(l)} + n_h^{(l)} - C(x), \quad \delta V(0) = \delta V(1) = 0,$$

where $n_h^{(l)} = n(V_h^{(l)}, w_{1h}^{(l+1)}, w_{2h}^{(l+1)})$ and the functions $w_{1h}^{(l+1)}, w_{2h}^{(l+1)}$ are the solutions of the previous flux subsystem. Then we set $V_h^{(l+1)} = V_h^{(l)} + \delta V$. If $\|\delta V\|_2$ is smaller than a prescribed tolerance and if the right-hand side in (2.4) is small enough we stop the Gummel iteration and increase the applied voltage again to start the next Gummel iteration.

Remark. The coefficients of \mathbf{A}_h can be easily computed since, on (x_{i-1}, x_i) , we have

$$(2.5) \quad \frac{1}{h} \int_{x_{i-1}}^{x_i} e^{-(\bar{w}_{1h} - \bar{V}_h \bar{w}_{2h})} dx = e^{-(\bar{w}_{1h} - \bar{V}_h \bar{w}_{2h})}.$$

One might think that a better approximation of \mathbf{A} is obtained by taking the linear interpolants of V_h, w_{1h}, w_{2h} in the exponent. Denoting by J_h the linear interpolant operator, one could choose

$$(2.6) \quad \frac{1}{h} \int_{x_{i-1}}^{x_i} e^{-(J_h(w_{1h}) - J_h(V_h) \bar{w}_{2h})} dx$$

or

$$(2.7) \quad \frac{1}{h} \int_{x_{i-1}}^{x_i} e^{-(J_h(w_{1h}) - J_h(V_h) J_h(w_{2h}))} dx.$$

The integral (2.6) can be computed explicitly since the exponent is a linear function. However, we observed that the approximation (2.6) requires much more nodes than (2.5) to ensure the convergence of the iterative system. On the other hand, (2.7) needs to be calculated numerically. This can be done, for instance, with the functions

$$F_+(x) = e^{x^2} \int_0^x e^{-t^2} dt \quad \text{and} \quad F_-(x) = e^{-x^2} \int_0^x e^{t^2} dt, \quad x \in \mathbb{R}.$$

The mapping F_- is referred to as the *Dawson function* and can be approximated efficiently with Chebyshev polynomials and asymptotic expansions [11]. For both (2.5) and (2.7) the same number of nodes can be taken. The approximation (2.7) leads to a slightly faster convergence of the Gummel iteration compared to (2.5),

but every iteration step is more time consuming. Therefore, we have chosen the simple formula (2.5). \square

3. Numerical results for ballistic diodes

As numerical examples we simulate two n^+nn^+ ballistic diodes. In the first example, we choose the same numerical data as in [6]. More precisely, the device length is $0.6\ \mu\text{m}$ and the doping profile $C(x)$ equals $2 \cdot 10^{15}\ \text{cm}^{-3}$ for $x \in (0.1\ \mu\text{m}, 0.5\ \mu\text{m})$ (channel or n region) and $5 \cdot 10^{17}\ \text{cm}^{-3}$ elsewhere (n^+ regions). The ambient temperature is 300 K, the relaxation time $\tau_0 = 0.4$ ps, and the applied voltage $U = 1.5$ V. The computations are performed on a uniform grid with 101 nodes. (We notice that the scheme also works for 40 nodes.)

In Figure 1 the electron temperature T und electron mean velocity $u = I_1/qn$ (q being the elementary charge) are displayed. The electrons are moving from right to left. They heat up in the channel region and are close to the ambient temperature in the n^+ regions. The mean velocity shows a small velocity overshoot around $x = 0.14\ \mu\text{m}$. The maximal temperature equals $T_{\max} = 2348$ K and the maximal velocity is $u_{\max} = 1.404 \cdot 10^7$ cm/s. These values are in very good agreement with the results of [6], where $T_{\max} = 2330$ K and $u_{\max} = 1.44 \cdot 10^7$ cm/s have been reported.

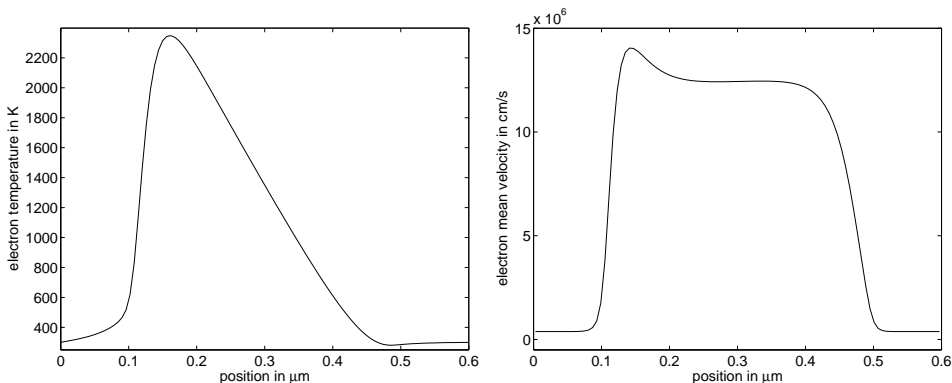


FIGURE 1. Electron temperature (left) and mean velocity (right) versus position in a ballistic diode with channel length $0.4\ \mu\text{m}$.

As a second example we present the temperature and mean velocity of a ballistic diode with channel length of 90 nm (Figure 2). The length of the n^+ regions is also 90 nm such that the total length of the device equals 270 nm. The physical parameters are the same as in the first example but the applied voltage is now $U = 1$ V. As expected, the temperature is smaller than in the first example since the voltage and the channel length are smaller. The overshoot of the mean velocity almost vanishes.

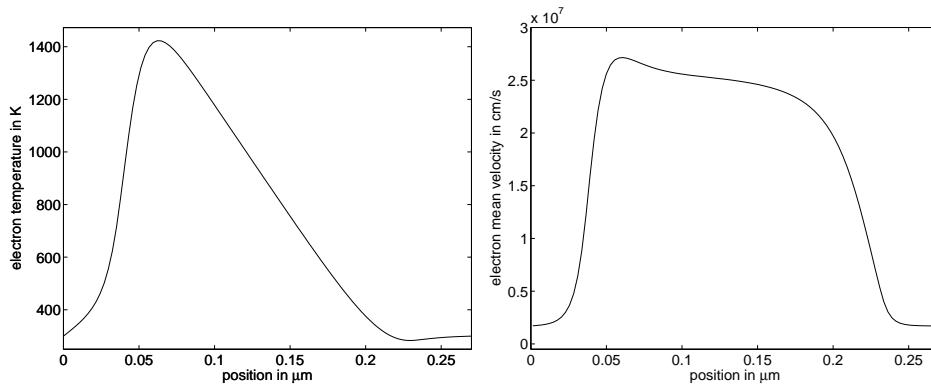


FIGURE 2. Electron temperature (left) and mean velocity (right) versus position in a ballistic diode with channel length 90 nm.

h	$\text{RE}(V_h)$	$\text{CR}(V_h)$	$\text{RE}(n_h)$	$\text{CR}(n_h)$	$\text{RE}(T_h)$	$\text{CR}(T_h)$
$2 \cdot 10^{-2}$	0.1819	—	0.6591	—	0.3858	—
$1 \cdot 10^{-2}$	0.0639	1.5089	0.2358	1.4828	0.1367	1.4968
$6.67 \cdot 10^{-3}$	0.0348	1.5027	0.1285	1.4965	0.0745	1.4980
$5 \cdot 10^{-3}$	0.0226	1.5015	0.0835	1.4977	0.0484	1.4990

TABLE 1. Relative errors and convergence rates for V_h, n_h, T_h .

In Table 1 we present, for the first example, the relative errors

$$\text{RE}(u_h) = \frac{\|u_h - u^*\|_{L^2}}{\|u^*\|_{L^2}},$$

where u_h is some numerical solution and u^* the reference solution, and the numerical convergence rates CR for the potential, the particle density, and temperature. For this, we have employed piecewise linear interpolation of the Lagrange multipliers $V_h, w_{1h},$ and w_{2h} . The reference solution is the numerical solution obtained on a very fine mesh with $h = 0.33 \cdot 10^{-4}$. We observe that the convergence rates are around 1.5 which is in good agreement with the results of [6].

References

- [1] G. Albinus. A thermodynamically motivated formulation of the energy model of semiconductor devices. Preprint No. 210, WIAS Berlin, Germany, 1995.
- [2] N. Ben Abdallah and P. Degond. On a hierarchy of macroscopic models for semiconductors. *J. Math. Phys.* 37 (1996), 3308-3333.
- [3] F. Bosisio, R. Sacco, F. Saleri, and E. Gatti. Exponentially fitted mixed finite volumes for energy balance models in semiconductor device simulation. In: H. Bock et al. (eds.), *Proceedings of ENUMATH 97*, World Scientific, Singapore, (1998), 188-197.

- [4] D. Chen, E. Kan, U. Ravaioli, C. Shu, and R. Dutton. An improved energy transport model including nonparabolicity and non-Maxwellian distribution effects. *IEEE Electr. Dev. Letters* 13 (1992), 26-28.
- [5] P. Degond, S. Génieys, and A. Jüngel. A system of parabolic equations in nonequilibrium thermodynamics including thermal and electrical effects. *J. Math. Pures Appl.* 76 (1997), 991-1015.
- [6] P. Degond, A. Jüngel, and P. Pietra. Numerical discretization of energy-transport models for semiconductors with nonparabolic band structure. *SIAM J. Sci. Comput.* 22 (2000), 986-1007.
- [7] A. Forghieri, R. Guerrieri, P. Ciampolini, A. Gnudi, M. Rudan, and G. Baccarani. A new discretization strategy of the semiconductor equations comprising momentum and energy balance. *IEEE Trans. Comp. Aided Design Integr. Circuits Sys.* 7 (1988), 231-242.
- [8] M. Fournié. Numerical discretization of energy-transport model for semiconductors using high-order compact schemes. *Appl. Math. Lett.* 15 (2002), 727-734.
- [9] S. Holst, A. Jüngel, and P. Pietra. A mixed finite-element discretization of the energy-transport equations for semiconductors. *SIAM J. Sci. Comput.* 24 (2003), 2058-2075.
- [10] S. Holst, A. Jüngel and P. Pietra. An adaptive mixed scheme for energy-transport simulations of field-effect transistors. *SIAM J. Sci. Comput.* 25 (2004), 1698-1716.
- [11] D.G. Hummer. Expansions of Dawson's function in a series of Chebyshev polynomials. *Math. Comp.* 18 (1964), 317-319.
- [12] J. Jerome and C.-W. Shu. Energy models for one-carrier transport in semiconductor devices. In: W. Coughran et al. (eds.), *Semiconductors, Part II*, New York, Springer, (1994), 185-207.
- [13] A. Jüngel. *Quasi-hydrodynamic Semiconductor Equations*. Birkhäuser, Basel, 2001.
- [14] C. Lab and P. Caussignac. An energy-transport model for semiconductor heterostructure devices: application to AlGaAs/GaAs MODFETs. *COMPEL* 18 (1999), 61-76.
- [15] L. D. Marini and P. Pietra. An abstract theory for mixed approximations of second order elliptic equations. *Mat. Applic. Comp.* 8 (1989), 219-239.
- [16] L. D. Marini and P. Pietra. New mixed finite element schemes for current continuity equations. *COMPEL* 9 (1990), 257-268.
- [17] A. Marrocco and P. Montarnal. Simulation de modèles "energy transport" à l'aide des éléments finis mixtes. *C. Rend. Acad. Sci. Paris* 323 (1996), 535-541.
- [18] A. Marrocco, P. Montarnal, and B. Perthame. Simulation of the energy transport and simplified hydrodynamic models for semiconductor devices using mixed finite elements. In: J. Desideri et al. (eds.), *Numerical Methods in Engineering '96*, Proceedings of ECCOMAS 96, John Wiley, London (1996), 645-650.
- [19] K. Souissi, F. Odeh, H. Tang, and A. Gnudi. Comparative studies of hydrodynamic and energy transport models. *COMPEL* 13 (1994), 439-453.
- [20] R. Stratton. Diffusion of hot and cold electrons in semiconductor barriers. *Phys. Rev.* 126 (1962), 2002-2014.

INSTITUT FÜR MATHEMATIK, JOHANNES GUTENBERG-UNIVERSITÄT MAINZ, STAUDINGERWEG 9,
55099 MAINZ, GERMANY

E-mail address: {gatau,juengel}@mathematik.uni-mainz.de

ISTITUTO DI MATEMATICA APPLICATA E TECNOLOGIE INFORMATICHE DEL CNR, VIA FERRATA 1,
27100 PAVIA, ITALY

E-mail address: pietra@imati.cnr.it